JMEPEG (2010) 19:1143–1149
DOI: 10.1007/s11665-010-9604-6

1059-9495/$19.00

Electrical and Thermal Properties of Twin-Screw Extruded Multiwalled Carbon Nanotube/Epoxy Composites

Jeena Jose Karippal, H.N. Narasimha Murthy, K.S. Rai, M. Krishna, and M. Sreejith

(Submitted April 24, 2009; in revised form November 11, 2009)

This paper presents the experimental results of dispersing multiwalled carbon nanotubes (MWNTs) into epoxy (space grade structural adhesive) nanocomposites using co-rotating twin screw extrusion process. Two sets of specimens were prepared; set 1 with ultrasonication for predispersing MWNT before extrusion and set 2 direct dispersion of MWNT in the extruder. MWNT was loaded up to 8 vol.% in both the sets. The specimens were characterized for room temperature volume and surface resistivities as per ASTM D257 using Keithley Model 6517 and for thermal conductivity in the temperature range −50 to 150 °C as per ASTM E 1530 using Thermal Conductivity Instrument (TCI) 2022 SX211. The volume resistivity of sets 1 and 2 decreased to an extent of 10^{11} and 10^{9} respectively. The surface resistivity drop was of the order of 10^{9} for both the sets. These drops corresponded to the maximum MWNT loading of 8 vol.%. Electrical conductivity values of the specimens were fitted into the Power Law Model to evaluate the critical exponent. Both sets 1 and 2 showed increase in thermal conductivity with increase in temperature in the testing range. Thermal conductivity increased with increase in filler loading and the maximum increase was 60% at 150 °C in case of 8 vol.% MWNT nanocomposites for set 1. The corresponding value for the set 2 was 25%. Thermal conductivity values were predicted using Lewis Nielson model. DSC of the specimens showed increase in glass transition temperature with increase in filler loading. The dispersion of the nanofillers was studied using SEM and the surface morphology using AFM.

Keywords electrical resistivity, extrusion, MWNT, thermal conductivity, ultrasonication

1. Introduction

Conductive polymer composites find use in electronics, automotive and aerospace systems. The outstanding properties of the CNTs make them promising filling materials for these applications. But the number of applications using these fillers is largely limited by their poor processibility. The intrinsic van der Walls attraction among the tubes in combination with their high surface area and high aspect ratio often leads to significant agglomeration of CNTs. The surface of CNTs is also non-reactive, which makes it difficult to achieve efficient dispersion, as they mix and blend with the host matrix.

Though several mechanical methods such as ultrasonication (Ref 1-7), magnetic agitation (Ref 8-10), screw extrusion (Ref 5), melt mixing (Ref 11) have been used to achieve the dispersion of CNTs in polymeric resins, the achieved conductivity results are varied and dependent on the resins, the filler quality, the process parameters, etc.

Jeena Jose Karippal, H.N. Narasimha Murthy, M. Krishna, and **M. Sreejith**, Department of Mechanical Engineering, R V College of Engineering, Bangalore 560059 Karnataka, India; and **K.S. Rai**, Department of Polymer Science, Mysore University, Mysore, Karnataka, India. Contact e-mail: hnmdatta@yahoo.com.

Nomenclature

MCNT	multiwalled carbon nanotube
σ_v	volume resistivity
ρ_s	surface resistivity
σ_{pc}	volume conductivity of polymer composite
v	volume fraction of the filler
v_c	critical volume fraction
K	thermal conductivity
ϕ	volume fraction
ϕ_m	maximum volumetric packing fraction of the filler
T_g	glass transition temperature

The main objective of this paper was to prepare MWNT/epoxy nanocomposites using twin screw extrusion process and characterize the same for electrical and thermal conductivity. The process involved two routes, the first using sonication for predispersing MWNT before extrusion and the second direct extrusion of the nanocomposites. The results of the two routes were compared experimentally.

2. Experimental

2.1 Materials

The resin used in this study consisted of modified Bisphenol-A based two component epoxy [Structural Adhesive-Araldite AV138M with modified Polyaminoamide Hardener

Table 1 Specifications of the MWNT

Material	Description	Properties	Suppliers (M/s)
MWNT	CVD grown grade: AP60-80/90	60-90 nm, 1-3 μm, purity > 90%	Nanovatec Chemapol Industries, Mumbai

HV998, (Huntsman, Hindustan Ciba-Geigy Ltd.)] and the filler was multi-walled carbon nanotube (Table 1).

2.2 Preparation of Nanocomposites

For dispersing the MWNT in epoxy, a co-rotating twin-screw extruder (OMEGA 20, M/s STEER Engg, Bangalore) was used. The process parameters evolved based on the viscosity of the resin were speed 200 rpm, temperature 60-75 °C, residence time 2-3 min. Two sets of samples were prepared for comparison. In set 1, MWNT was dispersed in acetone, ultrasonicated (27 kHz) for 1 h, epoxy resin was added and again sonicated for 1 h. The mix was processed using the twin-screw extruder in two passes. The hardener was added to the screw extruded mix and allowed to cure under room temperature for 1 week. The same process sequence was followed for preparing set 2 samples except the predispersion of MWNT in the solvent.

2.3 Electrical Resistivity Measurement

The volume and surface resistivities of the nanosamples were measured according to ASTM D257 using Keithley 6517A model 8009. The 3 mm thick and 75 mm diameter specimens were copper-plated for better contact after subjecting them to humidity conditioning at 95% RH and 37 °C. The resistivity values were calculated using the formula:

$$\sigma_v = \frac{22.9}{t} R \quad \text{(Eq 1)}$$

$$\rho_s = 53.4R \quad \text{(Eq 2)}$$

where σ_v and ρ_s are the volume and surface resistivities, R the corresponding resistance in ohms (meter reading), 22.9 and 53.4 the constants for the apparatus. The experimental values of electrical resistivities are presented in Fig. 1.

2.4 Thermal Conductivity Measurement

Thermal conductivity was measured using Thermal Conductivity Instrument (TCI) 2022 SX211 as per ASTM E 1530 under 10^{-5} Torr vacuum environment with measurement accuracy of ±3%. The 50 mm diameter and 10-mm-thick specimens were used for this study. To ensure good contact between the test samples and the flex meter, the surface finish of the sample were improved by working with a fine emery paper. The experimental results of the thermal conductivity in the temperature range −50 to 150 °C are presented in Fig. 3.

2.5 Morphological Characterization

Scanning electron microscope (JEOL JSM 840A, Japan) was used to study the dispersion of MWNT in the matrix in both the routes followed. The samples were examined with gold-sputtering for SEM characterization.

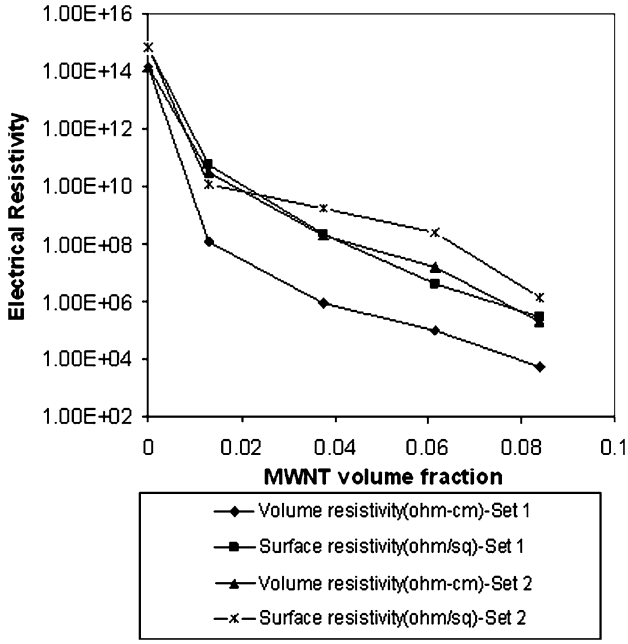

Fig. 1 Variation of electrical resistivity with MCNT volume fraction

2.6 Differential Scanning Calorimetry (DSC)

Glass transition temperature, T_g, of the specimens was obtained using DSC (Model Mettler DSC-823, temperature range 25-500 °C). The sample weighing 5 mg sealed in hermetic aluminum crucible was used for characterization. For obtaining the curing heat flow pattern of the composite, a dynamic scanning experiment was conducted from room temperature to 150 °C at a heating rate of 20 °C per minute in N_2 atmosphere (20 mL/min).

3. Results and Discussion

3.1 Electrical Resistivity

Room temperature electrical conductivity of the nanocomposites was measured to characterize the extent of the MWNT network. For set 1, low loading (<0.02 volume fraction) samples displayed a significant 10^6 drop in volume resistivity and the same drop for set 2 was 10^4. The critical volume concentration (percolation threshold where a sharp onset in conductivity occurs) at which a conductive path is formed in the composite causing the material to convert from a capacitor to a conductor was observed at 0.005 and 0.0075 volume fractions for sets 1 and 2, respectively. The lower percolation threshold for set 1 samples was attributed to the better dispersion of the filler due to its predispersion using ultrasonication. The value of the percolation threshold is very sensitive to the polymer type, filler and the dispersion process. Experimental results of similar studies have been summarized in Table 2. The viscosities of the epoxy resins used in these studies are much lower than that of AV138M (200-700 Pa·s) used in the present study. The higher the viscosity of the resin, the greater the issues in the dispersion of MWNT (Ref 6). To overcome this, the nanocomposites were processed using screw extrusion with sonication for the set 1 and only extrusion for set 2

Table 2 Elsewhere studies of fillers, resins, dispersion routes, and percolation and conductivity achieved

	Filler geometrical factors	Process	v_c	Resistivity at max. filler loading, Ω·cm
Epoxy/MWNT (Ref 4)	D = 50 nm, L = 1-10 μm	Acetone/tergitol/sonication + rotating blade	0.04 volume fraction	10^6 (12 wt.%)
Epoxy/SWNT (Ref 2)	D = 3-30 nm, L = 100 nm to 5 μm	DMF/sonication	0.1-0.2 wt.%	…
Epoxy/VGCF (Ref 2)	D = 200 nm, L = 10 mm	DMF/sonication	1-2 wt.%	…
Epoxy/MWNT (Ref 13)	D = 10-80 nm, L = 80 μm	High speed stirrer (2000 rpm)	0.0025 wt.%	1.0 (0.5 wt.%)
Epoxy/SWNT (Ref 13)	D = 2 nm, L >= 10 μm	Ethanol/sonication	0.05 and 0.23 wt.%	10^1 and 10^3 (0.5 wt.%)
Epoxy/MWNT (Ref 8)	D = 15-400 nm, L = ~100 μm	Methanol/magnetic agitation	0.5-1 wt.%	10^{-1} (4 wt.%)
Epoxy/MWNT (Ref 14)	D = 20 nm, L = 10-50 μm	Ethanol/sonication	<0.5 wt.%	10^2 (1.5 wt.%)
Polyimide/SWNT (Ref 1)	D = 1.4 nm, L = 3 μm	DMF/sonication/stirring	0.05 vol.%	10^6 (1 vol.%)
Epoxy/AP-SWNT (Ref 3)	…	Acetone/sonication	0.04 vol.%	10^1 (4 vol.%)
Epoxy/ P-SWNT (Ref 3)	…	Acetone/sonication	1.0 vol.%	10^3 (7.5 vol.%)
Epoxy/MWNT (Ref 15)	D = 30-50 nm, L = 3 μm	Ultrasonic irradiation/mechanical stirrer	<0.1 wt.%	10^3 (0.4 wt.%)
HDPE/graphite flakes (Ref 16)	10-20 μm	Powder mixing	2 wt.%	10^2 (15 wt.%)
Epoxy/MWNT (this work)	D = 60-90 nm, L = 1-3 μm	Acetone/sonication/extrusion (set 1)	0.5 vol.%	10^3 (8 vol.%)
Epoxy/MWNT (this work)	D = 60-90 nm, L = 1-3 μm	Extrusion (set 2)	0.75 vol.%	10^5 (8 vol.%)

in the present study. Screw extrusion for nanocomposites processing using thermoset resins is not reported so far in the open literature and the present study demonstrates the adoption of twin-screw extrusion process which is basically designed for thermoplastics. The rotation of the twin screws and the elements of the kneading block develop sufficient shear to enable the nanofillers to disperse in the resin. Also, there is a combined effect of temperature due to the heating coils provided in the barrel and that due to the shear action, which tends to reduce the viscosity of the processing mix.

The volume resistivity of sets 1 and 2 decreased to an extent of 10^{11} and 10^9, respectively. The surface resistivity drop was of the order of 10^9 for both the sets. These drops corresponded to the maximum MWNT loading of 8 vol.% and are comparable with the results reported by others considering the viscosity of the resin used (Ref 3, 4). With the achieved values of volume resistivity of the nanocomposites, i.e. 10^3 Ω·cm for set 1 and 10^5 Ω·cm, the material becomes suitable for electrostatic discharge (ESD) or electromagnetic interference (EMI) shielding applications. It is reported that electrical resistivity of below 10^8 Ω·cm is needed in order to avoid the electrostatic charging of insulating matrix.

The volume conductivity data of sets 1 and 2 samples were fitted to a power law in terms of volume fraction of MWNT. The power law is described by the equation (Ref 1):

$$\sigma_{pc} = A(v - v_c)^t, \quad v > v_c \qquad \text{(Eq 3)}$$

where σ_{pc} is the conductivity of the composite, v is the volume fraction of nanofiller in the composite, v_c is the critical volume fraction (percolation threshold), A and t are fitted constants (Fig. 2). The geometrical particle anisotropy with a random distribution inside the matrix is a key factor for determining the percolation threshold.

The critical exponent t is dependent on the dimensionality of the system (t = 1-1.3 in two dimension, t = 1.6-2 in three dimension, and $t > 2$ have been observed in anisotropic systems) (Ref 12). Theoretically the value of constant A should approach the conductivity of the nanofillers. The value of A depends not only on the conductivity of CNT, but also on the aspect ratio (L/D) of CNT (Ref 12). The experimental values of A (Table 3) were found to be lower than the expected values for both sets 1 and 2 samples. This may be due to lack of physical contact between the nanofillers caused by the contact resistance between the adjacent nanofillers, which decreases the effective conductivity of the nanofillers. Moreover, in these composites, conducting fillers are separated by the insulating polymers that act as a potential barrier, so that it is likely that the electrical conductivity is limited by hopping and/or tunneling of the charge carriers between conductive fillers (Ref 1).

3.2 Thermal Conductivity

Both sets 1 and 2 specimens showed increase in thermal conductivity (K) with increase in temperature in the −50 to 150 °C range and the filler loading as shown in Fig. 3. In the measured temperature range, the K values of the samples increased linearly. Between −50 and +50 °C the increase is linear and stable. Beyond +50 °C a sudden increase in the measured value of K was observed, which may be due to some thermal activity of the samples tested. The maximum increase in K for set 1 was 60% at 150 °C in case of 8 vol.% MWNT nanocomposites compared to that of neat resin. The corresponding value for set 2 was 25%. The K values obtained for

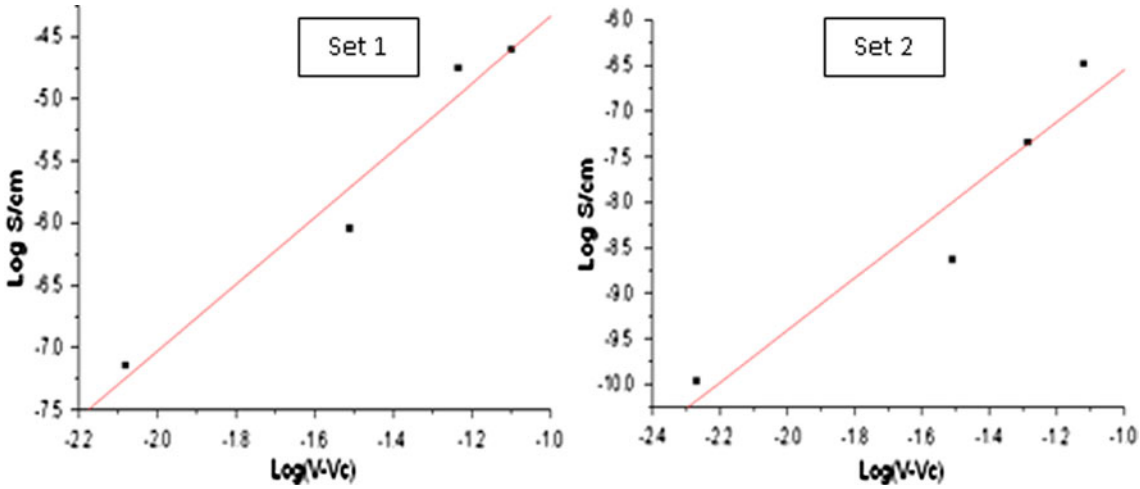

Fig. 2 Percolation equation fit to the conductivity data for sets 1 and 2

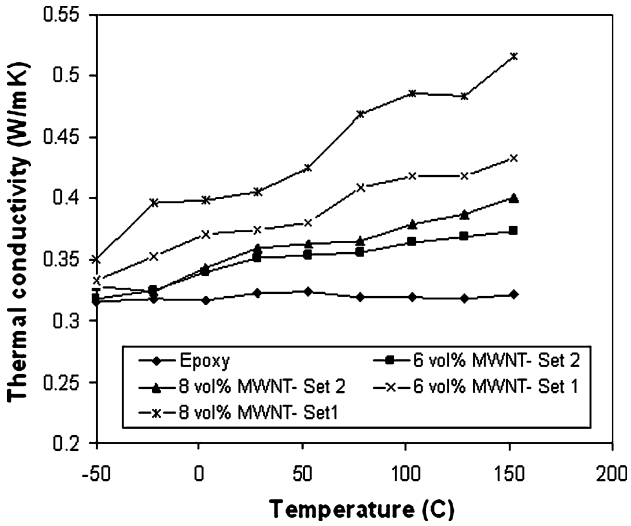

Fig. 3 Thermal conductivity of the composites with different volume fractions of MWNT at different temperatures

Table 3 Power law equation parameters

Parameter	Set 1	Set 2
t	2.6	2.8
A	5.43×10^{-2}	3.27×10^{-4}

set 1 at 6 vol.% MWNT were greater than that corresponding to 8 vol.% MWNT for set 2 in the measured temperature range. The superior K values for set 1 are attributed to the predispersion of MWNT using ultrasonication enabling breaking of the CNT agglomerates.

In contrast to the electrical conductivity (σ) behavior, percolation threshold for thermal conductivity (K) was not observed in the specimens. The increase in electrical conductivity achieved was very high, i.e. extents of 10^{11} and 10^{9} for sets 1 and 2 respectively corresponding to MWNT loading of 8 vol.%. But in the thermal transport, the increase in K was only by 60 and 25% for sets 1 and 2 respectively for MWNT loading of at 8 vol.% at room temperature. This is because

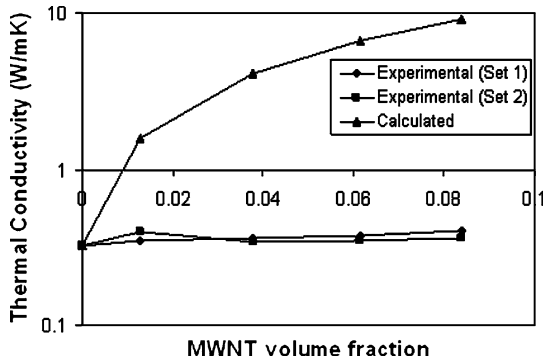

Fig. 4 Thermal conductivity of MWNT composites at room temperature

of the significantly greater values of $\sigma_{filler}/\sigma_{matrix}$ (10^{12}-10^{16}) than K_{filler}/K_{matrix} (10^{4}) for epoxy and MWNT systems. With high ratios the only effective channel for the electric transport is along the percolation network, but for thermal transport the main channels of heat flow always involve the matrix. In addition, the large thermal interface resistance of matrix to the heat flow at the MWNT junctions causes significant reduction in thermal conductivity increase of nanocomposites (Ref 3, 14, 17).

The thermal conductivity of the specimens was calculated using the Lewis-Nielsen model. According to this model, the thermal conductivity of a two-phase system (a non-conductive matrix and conductive filler) is given by the equations (Ref 9):

$$\frac{K}{k_1} = \frac{1 + A \times B \times \phi_2}{1 - B \times \psi \times \phi_2} \quad \text{(Eq 4)}$$

$$B = \frac{k_2/k_1 - 1}{k_2/k_1 + A} \quad \text{(Eq 5)}$$

$$\psi \cong 1 + \frac{1 - \phi_m}{\phi_m^2}\phi_2 \quad \text{(Eq 6)}$$

In Eq 4-6, K is the thermal conductivity of the composite and k_i is the thermal conductivity of the component i. In the

Table 4 Theoretical and experimental data of thermal conductivity of MWNT filled composites at room temperature

MWNT, vol.%	Experimental thermal conductivity, W/mK		Predicted thermal conductivity, W/mK	*A*	*B*	ψ
	Set 1	Set 2				
0	0.322	0.322	0.322	330	0.90	1.00
1	0.352	0.339	1.57	330	0.90	1.02
3	0.359	0.343	4.08	330	0.90	1.07
6	0.374	0.351	6.59	330	0.90	1.11
8	0.405	0.359	9.12	330	0.90	1.14

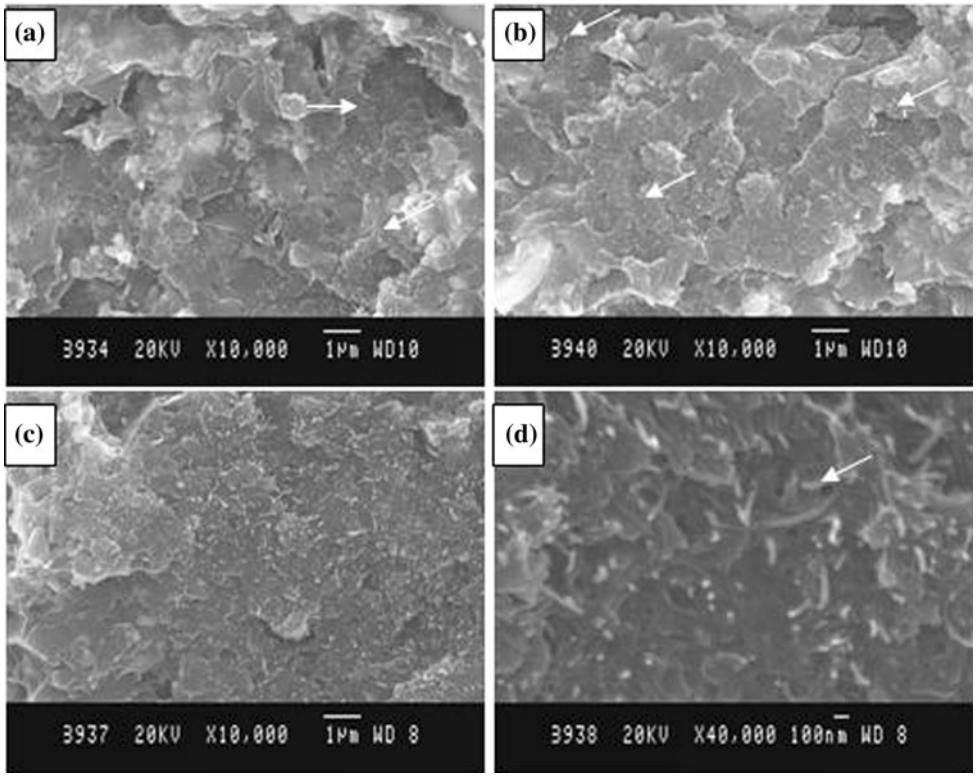

Fig. 5 SEM of MWNT/epoxy composites. (a) 6 vol.% MWNT/epoxy (set 2), (b) 8 vol.% MWNT/epoxy (set 2), (c, d) 8 vol.% MWNT/epoxy (set 1)

model, the subscript 1 represents the polymer matrix and 2 represents the filler. The parameter A in this equation accounts for the aspect ratio of the filler and ϕ_m describes the maximum volumetric packing fraction of the filler.

The experimentally measured and theoretically predicted thermal conductivity of the composites with different MWNT volume fractions are shown in Fig. 4 and Table 4. The values used for the calculation of other parameters in the model are listed in Table 4.

Experimental thermal conductivity values were far below than the predicted values using Lewis-Nielsen model. This may be due to the large number of junctions among carbon nanotubes to form a single conducting path. For sufficiently small particles, the properties of the polymer/nanoparticle interface also control the thermal transport in the composites. Another reason for the deviation in the predicted values may be the applicability of the model for nanolevel fillers as it is basically developed for macrolevel fillers (Ref 9).

3.3 Morphological Characterization

3.3.1 Scanning Electron Microscopy (SEM). To study the dispersion of MWNT in the epoxy matrix, the fracture surfaces of the samples were observed by SEM (Fig. 5). MWNT agglomerates can be observed in Fig. 5(a) and (b) as indicated by the arrows; good dispersion is seen in Fig. 5(c) and (d) which correspond to set 1 with 8 vol.% filler loading. This indicates that the predispersion of MWNT before extrusion resulted in better dispersion of MWNT in the matrix which is further proved by the electrical conductivity results.

3.3.2 Atomic Force Microscope (AFM). The compositional mapping with AFM is often used for observation of multiple phases. The phase contrast is related to the inherent properties of the two phases. The brighter areas in the image can be attributed to the greater force experienced by the cantilever tip when in contact with the filler (tubular or spherical). The matrix is in amorphous state and hence appears

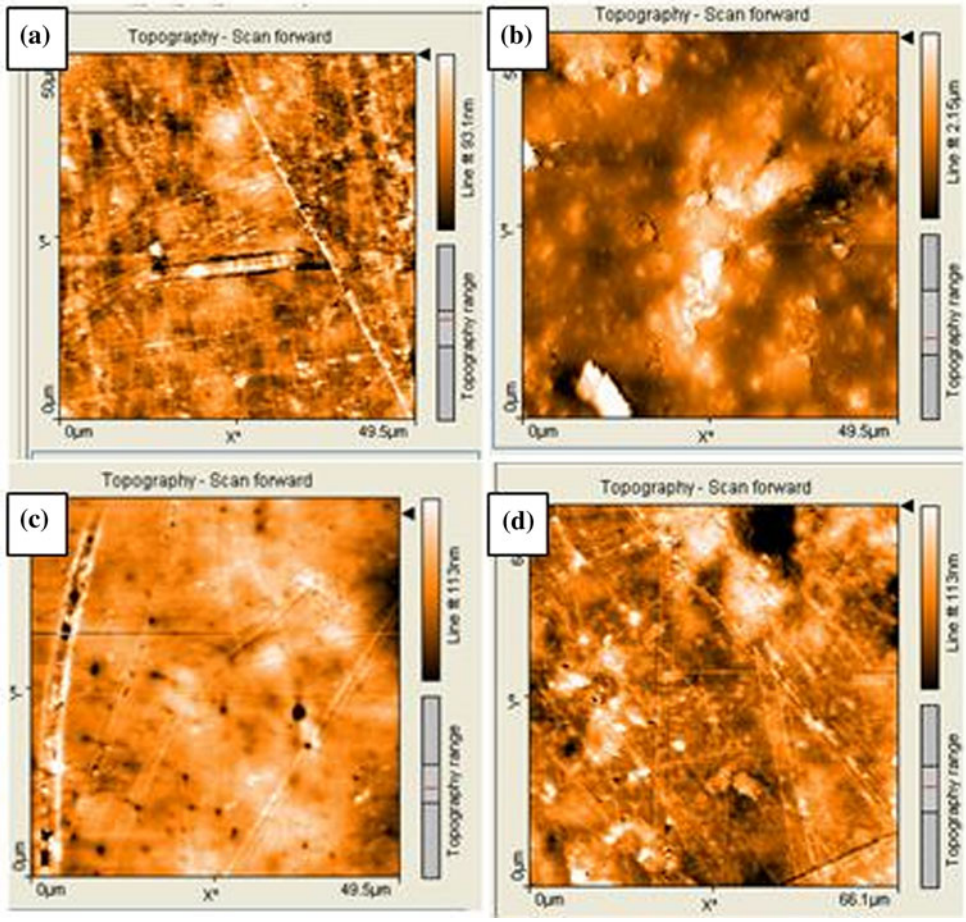

Fig. 6 AFM of MWNT/epoxy composites. (a) 6 vol.% MWNT/epoxy (set 2), (b) 8 vol.% MWNT/epoxy (set 2), (c) 6 vol.% MWNT/epoxy (set 1) and (d) 8 vol.% MWNT/epoxy (set 1)

dark in the images. CNT agglomerates are seen in samples of set 2 as indicated in the micrographs of Fig. 6(a) and (b). Micrographs of the samples with predispersion did not exhibit CNT agglomerates as shown by the well spread bright spots.

3.4 Differential Scanning Calorimeter

Differential scanning calorimeter was used to determine the T_g of the nanocomposites using the measurement of heat flow versus change in temperature. Figure 7 shows the variation of glass transition temperature with increase in MWNT loading. Whereas T_g increased with increase in MWNT in sets 1 and 2, the latter showed greater increase, which may be due to the use of solvent for the predispersion of the fillers (Ref 1). The addition of nanofillers enhanced the thermostability of the composites which may be due to the reduction in the mobility of the epoxy polymer chains around the nanofillers by strong interfacial interactions.

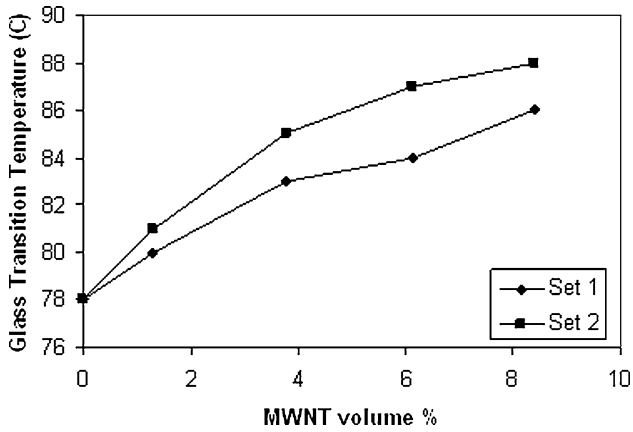

Fig. 7 Variation of glass transition temperature (T_g) with MWNT content

4. Conclusion

MWNT dispersed nanocomposites were fabricated with filler loading up to 8 vol.% using twin-screw extrusion process. The effect of predispersion of the nanofillers prior to extrusion was demonstrated in terms of greater reductions in electrical resistivity of the specimens. This was due to better dispersion of MWNT in the matrix which was confirmed by SEM and AFM. The experiments also demonstrated the adoption of extrusion process for thermoset-based nanocomposite preparation. The process parameters such as temperature, speed, and the screw elements can be fine-tuned for achieving better results. The decrease in electrical resistivity achieved with MWNT loading

was significant considering the nature of the resin system selected for the study. The experimental values of conductivity were described by a percolation-like power law equation with a percolation threshold of 0.005 and 0.0075 volume fractions for sets 1 and 2 respectively. Dispersion of MWNT resulted in increase in the thermal conductivity of the specimens. The specimens showed greater thermal stability as reflected by the increase in their glass transition temperature.

Acknowledgments

The authors are grateful for the financial support provided by the Indian Space Research Organization (ISRO), Bangalore (Sanction No. 10/3/547 dated 10-10-2005, Sanction Order No 9/2/125/2005 II dated 08-03-2006, Principal Investigator: Dr. H N Narasimha Murthy).

References

1. Z. Ounaies, C. Park, K.E. Wise, E.J. Siochi, and J.S. Harrison, Electrical Properties of Single Wall Carbon Nanotube Reinforced Polyimide Composites, *Compos. Sci. Technol.*, 2003, **63**, p 1637–1646
2. M.J. Biercuk, M.C. Llaguno, M. Radosavljevic, J.K. Hyun, and A.T. Johnson, Carbon Nanotube Composites for Thermal Management, *Appl. Phys. Lett.*, 2002, **80**, p 2767
3. A. Yu, M.E. Itkis, E. Bekyarova, and R.C. Haddon, Effect of Single-Walled Carbon Nanotube Purity on the Thermal Conductivity of Carbon Nanotube-Based Composites, *Appl. Phys. Lett.*, 2006, **89**, p 133102
4. S. Cui, R. Canet, A. Derre, M. Couzi, and P. Delhaes, Characterization of Multiwalled Carbon Nanotube and Influence of Surfactant in the Nanocomposite Processing, *Carbon*, 2003, **41**, p 797–809
5. E.T. Thostenson and T.-W. Chou, Aligned Multi-Walled Carbon Nanotube-Reinforced Composites: Processing and Mechanical Characterization, *J. Phys. D: Appl. Phys.*, 2002, **35**(16), p L77–L80
6. Y.-K. Choi, K.-i. Sugimoto, S.-M. Song, Y. Gotoh, Y. Ohkoshi, and M. Endo, Mechanical and Physical Properties of Epoxy Composites Reinforced by Vapor Grown Carbon Nanofibers, *Carbon*, 2005, **43**, p 2199–2208
7. Y.-H. Liao, M.-T. Olivier, L. Zhiyong, Z. Chuck, and W. Ben, Investigation of the Dispersion Process of SWNTs/SC-15 Epoxy Resin Nanocomposites, *Mater. Sci. Eng. A*, 2004, **385**, p 175–181
8. A. Allaoui, S. Bai, H.M. Cheng, and J.B. Bai, Mechanical and Electrical Properties of a MWCNT/Epoxy Composite, *Compos. Sci. Technol.*, 2002, **62**, p 1993–1998
9. Y. Xu, G. Ray, and B. Abdel-Magid, Thermal Behavior of Single-Walled Carbon Nanotube Polymer-Matrix Composites, *Composites A*, 2006, **37**(1), p 114–121
10. F.H. Gojny, H.G.W. Malte, B. Fiedler, and K. Schulte, Influence of Different Carbon Nanotubes on the Mechanical Properties of Epoxy Matrix Composites—A Comparative Study, *Compos. Sci. Technol.*, 2005, **65**, p 2300–2313
11. J.R. Hagerstrom and S.L. Greene, *Electrostatic Dissipating Composites Containing Hyperion Fibril Nanotubes*, Commercialization of Nanostructured Materials, Miami, USA, 2000
12. N. Hu, Z. Masuda, C. Yan, H. Fukunaga, and T. Hashida, Electrical Properties of Polymer Nanocomposites with Carbon Nanotube Fillers, *Nanotechnology*, 2008, **19**(215701)
13. A. Moisala, Q. Li, I.A. Kinloch, and A.H. Windle, Thermal and Electrical Conductivity of Single- and Multi-Walled Carbon Nanotube-Epoxy Composites, *Compos. Sci. Technol.*, 2006, **66**(10), p 1285–1288
14. Y.S. Song and J.R. Youn, Influence of Dispersion States of CNTs on Physical Properties of Epoxy Nanocomposites, *Carbon*, 2005, **43**(7), p 1378–1385
15. Y.X. Zhou, P.X. Wu, Z.Y. Cheng, J. Ingram, and S. Jeelani, Improvement in Electrical, Thermal Properties of Epoxy by Filling Carbon Nanotube, *eXPRESS Polym. Lett.*, 2008, **2**(1), p 40–48
16. S. Bhattacharya, V.K. Sachdev, and R.P. Tandon, Electrical Properties of Graphite Filled Polymer Composites, *2nd National Conference Mathematical Techniques: Emerging Paradigms for Electronics and IT Industries*, MATEIT, 2008
17. N. Shenogina, S. Shenogin, L. Xue, and P. Keblinski, On the Lack of Thermal Percolation in Carbon Nanotube Composites, *Appl. Phys. Lett.*, 2005, **87**, p 133106